Adaptive Centralized Random Access for Collision Free Wireless Local Area Networks

Adaptive Centralized Random Access for Collision Free Wireless Local Area Networks

Jinho D. Kim, David I. Laurenson, and John S. Thompson, *Fellow, IEEE*

***Abstract*—Packet collisions caused by the standard Distributed Coordination Function (DCF) protocol in wireless local area networks (WLANs) have been a challenging problem leading to congestion and reduced throughput. To solve this problem, we propose a novel backoff state generation algorithm, called adaptive virtual backoff algorithm (AVBA), operating in an access point. The virtual contention window size in the algorithm is automatically adjusted based on the number of synchronized active nodes in a cell. Backoff counts generated by AVBA operating in the access point are sent by the access point to each active node in the cell to try to synchronise transmissions and minimize packet collisions. Evaluation results show that AVBA improves the throughput performance compared to existing collision resolution techniques, such as deterministic backoff and centralized random backoff (CRB), when the number of active nodes is large. Moreover, the results show that it maintains a high level of fairness in terms of channel access opportunities between nodes using AVBA and nodes using the DCF protocol when they coexist in a mixed wireless network scenario.**

***Index Terms*—Medium access control, MAC protocol, wireless local area network, packet collision, random access, resource scheduling, collision resolution, and fairness.**

I. Introduction

Applications operating on wireless devices are extremely varied, and they are generally uncorrelated with each other. Fig. 1 shows a typical wireless network, where Wi-Fi devices follow the IEEE 802.11 standard Medium Access Control (MAC) protocol to transmit signals fairly on the frequency channel that the devices share. The standard MAC protocol employs the Distributed Coordination Function (DCF) method as a primary multiple access mechanism, which implements *random access* to the channel. The distributed random access protocol is simple to implement, and effective for maintaining fairness in terms of channel access opportunities between Wi-Fi users with various applications that share the same unlicensed frequency channel. A huge number of Wi-Fi devices using this multiple access technique have already been widely deployed, and new medium access techniques for local wireless communications in the unlicensed frequency bands must be capable of fairly coexisting with legacy Wi-Fi devices. These not only include communications by brand new Wi-Fi devices, but also include communications by LTE (Long-Term Evolution) devices operating in the unlicensed frequency bands.

J. D. Kim is with Hyundai Motor Company, South Korea. D. I. Laurenson and J. S. Thompson are with the Institute for Digital Communications (IDCOM) in School of Engineering, the University of Edinburgh, EH9 3JL, Scotland, United Kingdom.
E-mails: jinho.kim.uoe@gmail.com; dave.laurenson@ed.ac.uk; john.thompson@ed.ac.uk

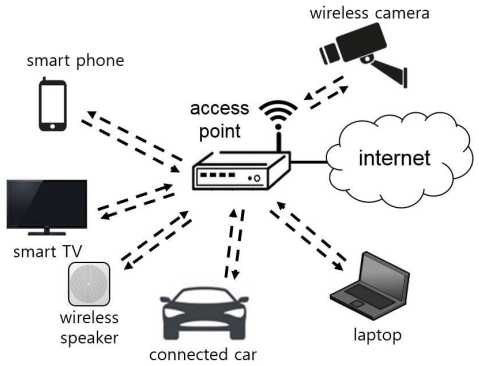

Fig. 1: A wireless local area network with a diversity of applications.

In a wireless local area network (WLAN) using the DCF protocol, two or more independent active nodes can reach backoff count zero at the same time, and simultaneous transmissions from such nodes can occur. The transmitted data signals can interfere with each other, and the result may be that none of the transmitted signals is successfully received. This undesirable event is called a *packet collision*. The packet collision issue will become more critical in future, because it is anticipated that the number of active nodes, n, served by a wireless network will increase. Recently, the 802.11ah standard technology was developed to enable long range wireless local area networks (e.g. up to 1.5 km) with lots of wireless sensor devices, and the 802.11ax standard task group considered how to improve average spectral efficiency in a dense user environment. Both standardization approaches assume that the number of nodes served by a wireless network will increase. However, these wireless technologies will still mainly be based on the DCF protocol.

In the past, a large number of ideas were proposed for reducing the probability of a packet collision [1], [2]. However, the packet collision probability, p, is still larger than zero in such methods, and this still causes performance degradation. Recently, new approaches have been reported for achieving *collision free* WLANs, where the collision probability p can approach zero [3]–[15]. These methods involve stations announcing their randomly chosen backoff count to assist neighbouring nodes to choose non-conflicting backoff counts [3], adaptively choosing a backoff count based on historical use by other nodes [4], or using a deterministic backoff

algorithm that ensures an exclusive backoff count for each node [5]–[13].

The concept of centralized random backoff (CRB) was proposed in [14], and it was further evaluated in [15]. In the CRB method, backoff states are generated by a *virtual backoff algorithm* (VBA) operating in the AP (Access Point), and they are allocated to the connected active nodes by means of ACK frames. So, the operation of medium access control in the network is defined by the allocated backoff states, and the network converges to a collision free state after a *convergence time*. The concept of a *virtual collision* in VBA was created to allow the access point to ensure that each node is allocated a unique backoff state. (A virtual collision in VBA is the event that a selected random number in VBA is the same as the backoff count of another synchronized node in the network.) It was reported in [15] that a high level of fairness between CRB and DCF nodes in terms of channel access opportunity is maintained when they coexist. In CRB, how active nodes access the shared channel is defined by the backoff state generation algorithm operating in the AP. Since APs normally maintain a reliable connection to the internet, such an algorithm can be updated easily on demand.

According to the IEEE 802.11 standards, only three rates (i.e. 6 Mbps, 12 Mbps, and 24 Mbps) are mandatory. This means one of the three rates has to be used for transmitting ACK frames in order to support backward compatibility. When the 6 or 12 Mbps rate is used for transmitting ACK frames, adding two additional octets for including the CRB field requires an additional OFDM symbol. This may be a small cost for implementing a centralized wireless network. If the 24 Mbps rate is used, it does not require an additional OFDM symbol.

A couple of limitations of CRB were shown in [15]. First, the throughput gain is reduced because of the *slow convergence speed* when the number of active nodes n is large. For example, a network with twenty active CRB nodes may take an hour to achieve a collision free state. Second, the level of fairness to legacy DCF nodes should be further improved. A large number of devices using the standard DCF protocol have been widely deployed, and a brand new device using a new medium access technique must fairly coexist with such legacy DCF devices in terms of channel access opportunity. Moreover, little attention has been paid to an adaptive control algorithm for CRB.

In order to tackle both the slow convergence speed and the level of fairness to legacy devices, we propose a novel backoff state generation algorithm, which is called the *adaptive virtual backoff algorithm* (AVBA). In CRB, it is observed that as the number of synchronized CRB nodes (SCNs) increases, the number of virtual collisions tends to increase; as the number of virtual collisions increases, the backoff state generation algorithm operating in the AP tends to generate a backoff state with a larger backoff count value. The AVBA has been designed based on these observations. The AP computes the average number of virtual collisions based on the number of SCNs, and the average number of virtual collisions is used to determine the adaptive virtual contention window size. The adaptive virtual contention window size in AVBA is then periodically adjusted.

Note that the number of SCNs is directly (and exactly) known to the AP at all times regardless of the number of stations n, while the number of nodes n is unknown to the AP. (Although the number of nodes n could be known to the AP indirectly by estimation techniques such as [16], [17], it is still a very complex issue because of slow adaptation when the number of active nodes n is large and changes rapidly.) Evaluation results show that AVBA is much faster than the CRB method in terms of convergence speed for achieving a collision free state (when legacy DCF nodes are not active/present). Moreover, it is fairer to legacy DCF nodes when coexisting with them.

Section II reviews related works. Section III summarizes the network model to be considered in this paper. Section IV recapitulates the concept of CRB, and then introduces the concept of AVBA. Section V presents analysis of throughput performance. Section VI shows simulation results. Section VII summarizes key findings in this research, and presents remaining issues and future work.

II. Related Works

The CRB method has advantages over EBA (Early Backoff Announcement) [3]. In CRB, backoff information is sent by an ACK frame, which is a unicast transmission (from the AP to the source node) and the backoff information could be encrypted if required for security. Such ACK frames are generally more robust than data frames. Moreover, each time slot in CRB is randomly reserved by the VBA mimicking the standard DCF protocol. This allows randomly distributed unreserved time slots over time (like empty time slots when using the DCF). This is necessary to support highly dense wireless networks with multiple APs. Although CRB might not maintain a collision free state (because of interference causing desynchronization), it can still operate in such a dense environment (like the standard DCF technique operating in such an environment).

The CRB technique achieves better performance than the deterministic backoff method studied in [5]–[13]. In the deterministic backoff method, nodes reserve a unique time slot through real packet collisions, while in CRB the nodes are allocated a unique time slot through *virtual collisions*, which only conceptually occur in the algorithm operating in the AP. Because of this difference, the network using CRB is more efficient without a dynamic parameter adjustment when the number of active nodes n is large. The modified deterministic backoff method discussed in [9] and [13] may not properly operate when the stations do not have a sufficient number of data packets in their transmission queue and/or when the channel condition varies rapidly. Moreover, transmitting a large number of data packets consecutively may cause a delay issue to nodes using a delay sensitive application or might also cause an unfairness issue when the number of active nodes varies over time in practical conditions such as multiple coexisting APs and/or in the presence of the hidden node problem.

III. System Model

We first consider a simple case where a single AP operates in the infrastructure mode as described in Fig. 1, and all nodes connected to the AP are assumed to follow the IEEE 802.11a physical layer standard. (AVBA to be discussed in this paper is also applicable to Wi-Fi devices using the IEEE 802.11b/g/n/ac standard techniques, as long as they follow the standard random access method for exchanging Data and positive ACK frames.) To derive a simple tractable analysis model for investigating this case, it is assumed that the network operates in saturated traffic conditions and all nodes are assumed to transmit User Datagram Protocol (UDP) packets, emulating real-time streaming applications, e.g. video telephony and screen mirroring applications. It implies the effect of queueing dynamics is very small. In the analysis model, we assume that interference from adjacent wireless networks is negligible. AVBA is also applicable when devices transmit transmission control protocol (TCP) packets; however, this specific topic is out of the research scope of this paper.

In order to test practicality of AVBA, we implement a Monte Carlo simulation based on the Network Simulator version 3.25 (NS-3.25) for more realistic cases such as unsaturated traffic conditions; the overlapping of two APs; a mixture of AVBA nodes and legacy DCF nodes; and a hidden node scenario. The Wi-Fi module of NS-3.25 source code implements the packet error rate (PER) model described in [18].

IV. Adaptive Virtual Backoff Algorithm

In this section, CRB [15] is briefly reviewed. Then, the concept of AVBA is introduced in detail.

A. Review of the Centralized Random Backoff (CRB)

In CRB, backoff states are generated by VBA operating in the AP, and they are allocated to stations by means of ACK frames. The pseudo-code shown in Fig. 4 in [15] describes how VBA generates a unique backoff state for each active station. In the figure, the scalar W_0 denotes the minimum contention window size defined in the 802.11 standard; the notation i represents the virtual backoff stage in the algorithm; the notation k represents the currently chosen virtual backoff count value in the algorithm; the scalar m is the maximum backoff stage value; the acronym *SBCs* stands for *synchronized backoff counts*, which are allocated backoff counts from the AP to active CRB nodes and are being used to access the channel. As seen in lines from 4 to 7 in the code, if a virtual collision occurs, then the value i increases by one and the algorithm selects a new random number from the doubled virtual contention window. If the newly selected number is unique compared to the SBCs, then it is allocated to the source node.

An active CRB node is either a *synchronized CRB node* (SCN) or an *unsynchronized CRB node* (UCN). An active CRB node that has been allocated a backoff state from the AP is called an SCN; an active CRB node that has not been allocated a backoff state and independently generates its backoff state (like a DCF node) is called a UCN. An active CRB node becomes an SCN after a successful transmission of a data frame and a successful reception of the ACK frame with the backoff state information. When the AP has data frames to send, the backoff state generation algorithm allocates a unique backoff state to the AP in order to avoid a collision with the SCNs. In this case, the active AP is considered as an SCN as well.

B. Adaptive Virtual Backoff Algorithm (AVBA)

The scalar $l(t)$ is defined as the number of SCNs at time t. The scalar $l(t)$ is an integer value in the range $[0, n]$. The AP computes and monitors the average number of synchronized nodes, $\tilde{l}(t)$, which can be expressed as (1).

$$\tilde{l}(t) = \lfloor \mathrm{Avg}(l(t)) \rceil \tag{1}$$

The notation $\lfloor x \rceil$ denotes the nearest integer from the value x, and the function $\mathrm{Avg}(l)$ denotes the simple moving average measured over the last 500 ms.

Fig. 2 describes how AVBA generates a backoff state. The notation W_0^a in the figure denotes the adaptive minimum contention window size $W_0^a(\tilde{l}(t))$, which is periodically adjusted depending on the average number of synchronized nodes $\tilde{l}(t)$. In contrast, the minimum contention window size in CRB, i.e. the value W_0 in lines 3 and 7 in Fig. 4 in [15], is a constant value regardless of the number of synchronized nodes. The value W_0^a is an integer larger than or equal to the value W_0. The relation between the minimum contention window size W_0 and the adaptive contention window size $W_i^a(\tilde{l}(t))$ at backoff stage i is given by equation (2),

$$W_i^a(\tilde{l}(t)) = 2^i \cdot \lfloor 2^{N_{vc}^{vba}(\tilde{l}(t))} \cdot \ W_0 \rceil \quad \text{where} \quad i \in [0, m]. \tag{2}$$

The function $N_{vc}^{vba}(l)$ is defined as the *average number of virtual collisions* per allocated backoff state when the number of SCNs using VBA is $l(t)$. The pseudo-code shown in Fig. 3 specifies the operation of AVBA in detail. Note that AVBA is based on the average number of synchronized nodes $\tilde{l}(t)$ (which is known to the AP at any time), and it only requires a minimal change from CRB. AVBA does not require an additional MAC frame exchange nor a technique to estimate the number of active nodes n.

1) The Average Number of Virtual Collisions : On average $N_{vc}^{vba}(l)$ virtual collisions occur in VBA before generating a unique backoff state when the number of synchronized nodes is l. From the Markov chain model studied in [15], the relation between the number of synchronized nodes, l, and the average number of virtual collisions per allocated backoff state $N_{vc}^{vba}(l)$ can be obtained as equation (3),

$$\begin{aligned} N_{vc}^{vba}(l) &= Q_0^l + Q_0^l Q_1^l + Q_0^l Q_1^l Q_2^l + \cdots + \prod_{k=0}^{m-2} Q_k^l \\ &\quad + \prod_{k=0}^{m-1} Q_k^l + \frac{\prod_{k=0}^{m} Q_k^l}{1 - Q_m^l} = \sum_{j=0}^{m-1} \prod_{k=0}^{j} Q_k^l + \frac{\prod_{k=0}^{m} Q_k^l}{1 - Q_m^l} \end{aligned} \tag{3}$$

where the notation Q_i^l denotes the probability of a virtual collision at virtual backoff stage i when the number of synchronized nodes is equal to l in VBA. (The probability

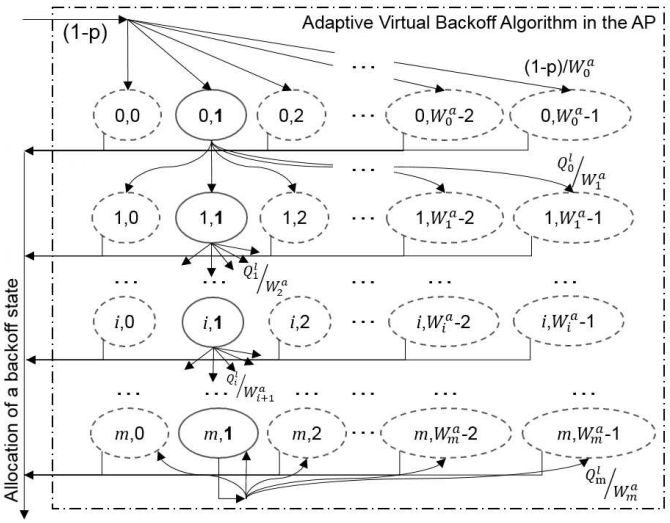

Fig. 2: The proposed adaptive virtual backoff algorithm (AVBA).

of a virtual collision, Q_i^l, is obtained by equations (1)-(6) in [15].)

The function $N_{vc}^{vba}(l)$ is shown in Fig. 4, where we see that as the number of synchronized nodes increases the average number of virtual collisions also increases. For example, the value $N_{vc}^{vba}(l)$ is approximately two when the value $l(t)$ is 35. This implies that, on average, three backoff counts are tested before sending a contention free backoff count value to a node when the number of synchronized nodes is 35, and it also implies that on average the unique backoff count value is selected in the range [0, $2^2 \cdot W_0 - 1$].

2) The Adaptive Contention Window Size: The adaptive contention window size $W_i^a(\tilde{l}(t))$ defined by equation (2) is obtained as the function $N_{vc}^{vba}(l(t))$ is given by equation (3). As the average number of synchronized nodes $\tilde{l}(t)$ increases, the value $W_0^a(\tilde{l}(t))$ also increases automatically in AVBA. This means as the average number of synchronized nodes $\tilde{l}(t)$ increases, AVBA tends to generate a larger backoff count value than a backoff count value generated by VBA. For example, given $W_0 = 16$ and $m = 6$, the adaptive minimum contention window size $W_0^a(\tilde{l}(t))$ becomes 26 when $\tilde{l}(t) = 10$ and it becomes 58 when $\tilde{l}(t) = 30$. This reduces the collision probability p when the number of active nodes n is large, and this reduces the convergence time for AVBA. By doing so, the total throughput gain when using AVBA is improved compared to VBA when n is large.

3) The Operation of Stations: The pseudo-code shown in Fig. 5 describes the operation of stations using AVBA. After a successful transmission, stations use the allocated backoff state to transmit the next data frame. (Refer to lines 9-10 in Fig. 5.) Lines from 2 to 7 in the pseudo-code describe the operation of AVBA nodes that have just become active. The operation of such active nodes are exactly the same as the operation of legacy nodes following the DCF protocol. This means that the nodes are assumed to be independent and distributed before a successful data frame transmission. Lines 11-15 describe the operation of a node after a transmission failure. Line 14 shows that the node selects a random number (as its backoff count) from the adaptive contention window size $W_0^a(\tilde{l}(t))$, not W_0. Use of the adaptive contention window size $W_0^a(\tilde{l}(t))$ after a transmission failure further reduces the convergence time of the network. Stations compute the adaptive contention window size $W_0^a(\tilde{l}(t))$ as follows. Each station operating using AVBA overhears data frames and ACK frames, and identifies the MAC addresses of them. It is assumed that the stations can distinguish ACK frames with a backoff state from overheard ACK frames. It is also assumed that the function $N_{vc}^{vba}(l(t))$ is known to the stations. Then, they can estimate the average number of synchronized nodes $\tilde{l}(t)$ connected to the AP, and they can compute the value $W_0^a(\tilde{l}(t))$.

V. NUMERICAL ANALYSIS

In this section, the operation of a node using AVBA is described with a Markov chain model, and the network converging to a collision free state is studied with linked absorbing Markov chains. Using the Markov chain model analysis, we investigate the relation between a convergence time period and total throughput performance of the wireless network.

A. Operation of a Node using AVBA

The operation of a node using AVBA can be expressed as a Markov chain model shown in Fig. 6. Unlike the Markov chain model for VBA presented in Fig. 11 in [15], this model for analysing AVBA consists of the adaptive contention window size $W_i^a(\tilde{l}(t))$ at backoff stage i. Since the structure of this model is identical to the structure of the Markov chain model in Fig. 11 in [15] (except the adaptive contention window size), this model can be solved by equations (10)-(17) in [15]. Note that this model becomes identical to the Markov chain model shown in [19] when the average number of synchronized nodes $\tilde{l}(t)$ is zero. This implies that the nodes tend to operate like legacy DCF nodes when the value $\tilde{l}(t)$ is small, and this implies that nodes using AVBA can fairly coexist with legacy DCF nodes when the proportion of nodes using AVBA is small in the mixed network.

B. Convergence to a Collision Free State

1) Settling Time After Adjustment: The network state changes before converging to a collision free state. The network state transition is described as follows. The AP monitors the average number of synchronized nodes $\tilde{l}(t)$, and determines the average number of virtual collisions $N_{vc}^{vba}(\tilde{l}(t))$. The AP periodically adjusts the adaptive virtual contention window size $W_i^a(\tilde{l}(t))$. For example, the AP shown in Fig. 7 adjusts the adaptive virtual contention window size at every time t_i. The time interval between adjustments is denoted by the notation Δt, i.e. $t_i - t_{i-1}$. Just after the virtual contention window size adjustment, some active nodes still use backoff count values allocated before the adjustment. For example, in Fig. 7, STA1 and STA2 are operating in the

1: **if** *a successful reception of a data frame* **then**
2: $i = 0$
3: $k = \text{rand}(0, 2^i \cdot W_0^a(\tilde{l}(t)) - 1)$ where $W_0^a(\tilde{l}(t)) = \lfloor 2^{N_{vc}^{vba}(\tilde{l}(t))} \cdot W_0 \rceil$
4: **while** k *is not unique compared to the SBCs (i.e. a virtual collision occurs)*
5: **if** $i < m$ **then**
6: $i = i + 1$
7: $k = \text{rand}(0, 2^i \cdot W_0^a(\tilde{l}(t)) - 1)$
8: Send the ACK frame with the backoff state (i, k)
9: **else**
10: Do not send an ACK frame

Fig. 3: The pseudo-code for AVBA operating in the AP.

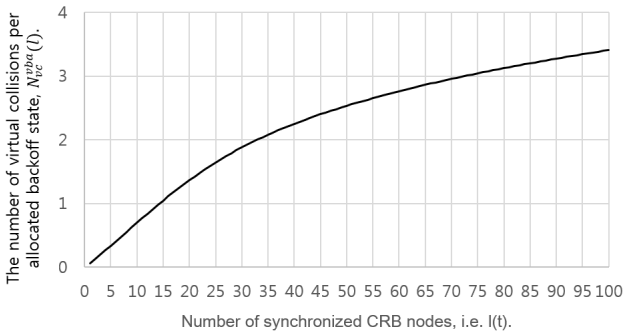

Fig. 4: The relation between the number of synchronized nodes l and the average number of virtual collisions $N_{vc}^{vba}(l)$ when using CRB.

backoff process with backoff count values that were allocated before the adjustment. The backoff counts being used by STA1 and STA2 were selected from a contention window size that is different to the contention window size used for STA3. At a later time for transmitting its next data frame, STA1 and STA2 will be allocated a backoff count selected from the updated contention window. We define the time period required for all the active nodes using AVBA in the network to use the same contention window size after the adjustment as a *settling time*. The settling time period ends once every node in the network successfully transmits a data frame to the AP and is allocated a backoff state from the AP.

2) Linked Absorbing Markov Chains: The convergence process to a collision free state can be described with the example of absorbing Markov chains shown in Fig. 8. In this example, it is assumed that the network starts from the initial state where $l(t) = 0$ and $W_0^a(\tilde{l}(t)) = W_0$. At the end of the first Δt time period, the measured average number of synchronized nodes $\tilde{l}(t)$ is equal to two for example. (Refer to ① in the figure.) Then, the AP adjusts the adaptive virtual contention window size to $W_0^a(\tilde{l}(t) = 2)$, and the network enters the settling time period. During the settling time period, the network operates in transitional mixed network states, where not all active AVBA nodes use a backoff count chosen with the same contention window size. (Refer to ② in the figure.) After the settling time period, it is assumed that all active AVBA nodes use the same contention window, and then the network state can be considered as one of network states in the 3rd absorbing Markov chain. (Refer to ③ in the figure.)

If provided a sufficient time period Δt after each adjustment of the parameter $W_0^a(\tilde{l}(t))$, the network state transitions between absorbing Markov chains can be approximated as the linked absorbing chain model shown in Fig. 9. In this regard, the value Δt is chosen as 500 ms in this analysis. This linked model expresses network state transitions occurring both every time slot (solid lines) and every adjustment time interval, i.e. Δt, (dotted lines). The notation j_a in Fig. 9 denotes the j-th time slot during which the adaptive contention window size is adjusted. Following this convergence process, the network state moves towards the absorbing state where $l = n$ and $p = 0$.

C. Saturation Throughput Analysis

1) The Number of Synchronized Nodes: We define the probability distribution vector P_i^j (where $i \in [0, n]$) as the probability distribution of the number of synchronized nodes l at the jth time slot when the network started from the network state where the average number of synchronized nodes $\tilde{l}(t)$ was equal to i. This vector P_i^j can be expressed as:

$$P_i^j = \begin{bmatrix} p_0^j(i) & p_1^j(i) & \cdots & p_{n-1}^j(i) & p_n^j(i) \end{bmatrix} \quad (4)$$

where each element $p_k^j(i)$ (where $k \in [0, n]$ and $i \in [0, n]$) denotes the probability that $l = k$ at the jth time slot from the time slot with a contention window size adjustment, where the number of synchronized nodes $\tilde{l}(t)$ was equal to i. The elements $p_k^j(i = 0)$ become equal to the elements p_k^j in the equation (18) in [15], because $W_0^a(\tilde{l}(t)) = W_0$ when $\tilde{l}(t) = 0$. Note that $\sum_{k=0}^{n} \sum_{i=0}^{n} p_k^j(i) = 1$.

The probability distribution vector P_i^j can be obtained by equation (5),

$$P_i^j = I_i \cdot (A_i)^j \quad (5)$$

where the vector I_i represents the network state that the number of synchronized nodes $\tilde{l}(t)$ is equal to i. For example, when $\tilde{l}(t) = 0$, the vector I_0 is equal to $\begin{bmatrix} 1 & 0 & 0 & \cdots & 0 & 0 \end{bmatrix}$ (i.e. the probability that $\tilde{l}(t) = 0$ is one, otherwise zero); in general when $\tilde{l}(t) = i$, only the $(i+1)$th element of the vector I_i is equal to one while all the other elements are zero, e.g. if $\tilde{l}(t) = 2$ then $I_2 = \begin{bmatrix} 0 & 0 & 1 & 0 & \cdots & 0 & 0 \end{bmatrix}$. In this analysis, the

1: **if** *Tx queue was empty, before a packet has arrived from upper layers* **then**
2: **if** *channel is sensed idle* **then**
3: Start transmitting immediately
4: **else** *channel is sensed busy*
5: $i = 0$
6: $k = \mathrm{rand}(0, 2^i \cdot W_0 - 1)$
7: Start backoff procedure with the state (i, k)
8: **else** *(this node has been active, i.e. saturation condition)*
9: **if** *a successful reception of a backoff state* (i, k) *from the AP* **then**
10: Start backoff procedure with the state (i, k)
11: **else**
12: **if** $i < m$ **then**
13: $i = i + 1$
14: $k = \mathrm{rand}(0, 2^i \cdot W_0^a(\tilde{l}(t)) - 1)$
15: Start backoff procedure with the state (i, k)

Fig. 5: The pseudo-code of the operation of a node using AVBA.

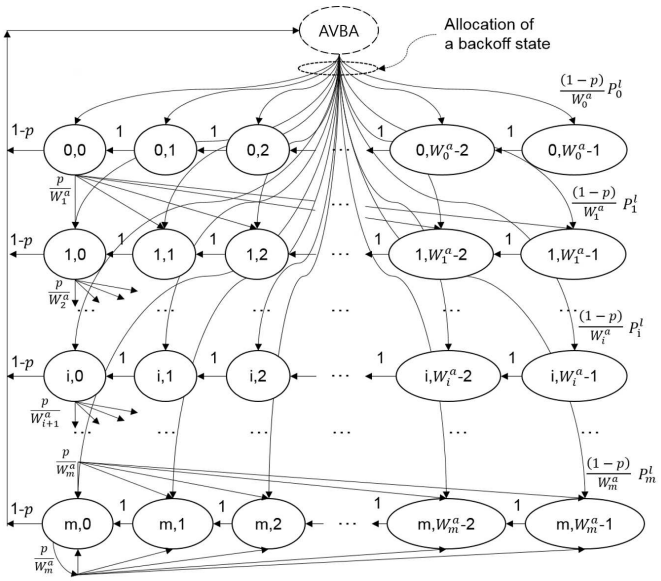

Fig. 6: Markov chain model of a node using AVBA.

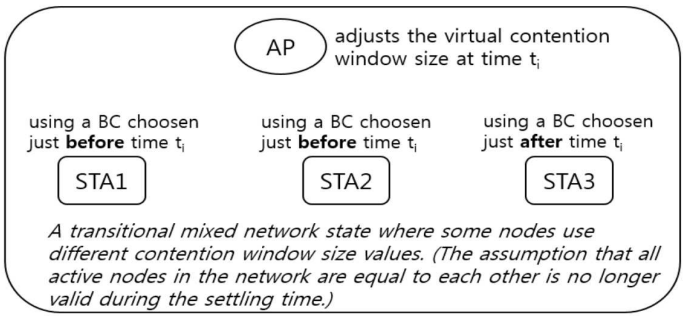

Fig. 7: An example of transitional mixed network state just after the adaptive contention window size adjustment.

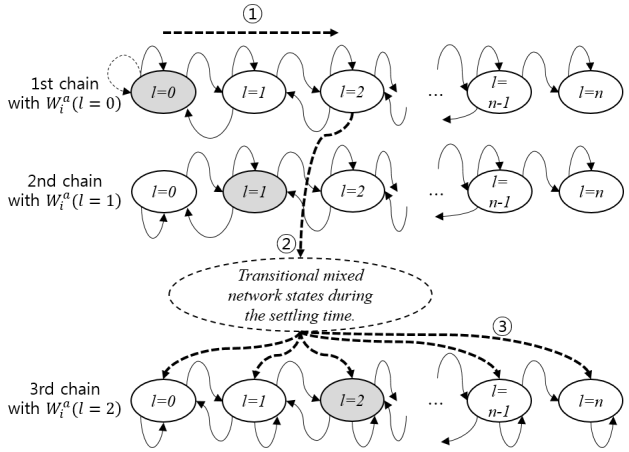

Fig. 8: An example of network state transition between absorbing Markov chains.

convergence time ends when the value of the element $p_n^j(i)$ in equation (4) exceeds 0.99.

2) Mathematical Expression for the Linked Absorbing Markov Chains: The matrix A_i in equation (5) represents the absorbing Markov chains shown in Fig. 9. Each of the linked absorbing chains shown in Fig. 9 starts with i synchronized nodes at the start of each Δt time period (i.e. the number of synchronized nodes $\tilde{l}(t)$ is equal to i when the AP adjusts the adaptive contention window size at the start of each Δt time period.). This matrix A_i can be expressed as (6),

$$A_i = \begin{bmatrix} S_{0,0}^i & S_{1,0}^i & 0 & \cdots & 0 & 0 \\ S_{0,1}^i & S_{1,1}^i & S_{2,1}^i & \cdots & 0 & 0 \\ 0 & S_{1,2}^i & S_{2,2}^i & \cdots & 0 & 0 \\ 0 & 0 & S_{2,3}^i & \cdots & 0 & 0 \\ \cdots & & & \cdots & \cdots & \\ 0 & 0 & 0 & \cdots & S_{n-1,n-1}^i & S_{n,n-1}^i \\ 0 & 0 & 0 & \cdots & 0 & S_{n,n}^i \end{bmatrix} \quad (6)$$

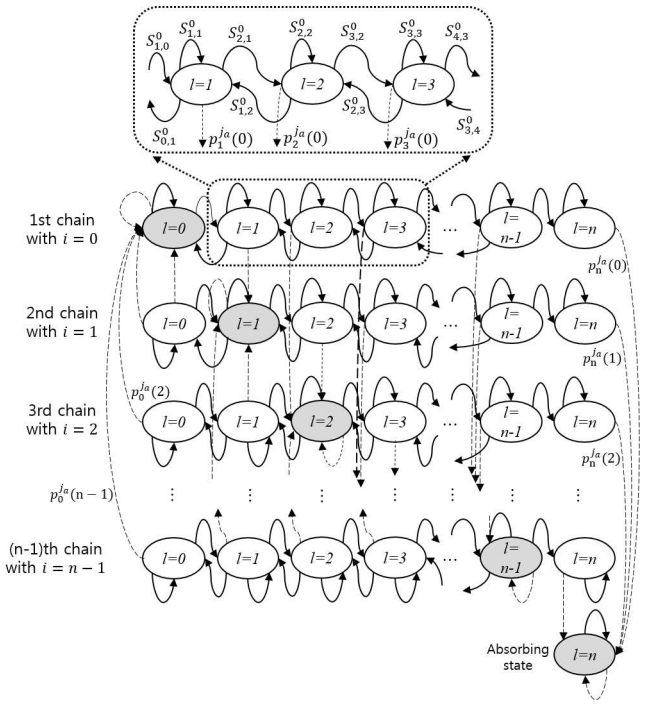

Fig. 9: Linked absorbing Markov chain model for describing the network state converging to a collision free state.

where each element $S^i_{x,y}$ represents the probability that the number of synchronized nodes changes from y to x during each Δt time period starting with $\tilde{l}(t) = i$.

3) Network Parameters: In order to obtain analytical results, the parameters shown in Table I are used. The choice of the value of the parameter Δt is important and is explained as follows. As the number of active nodes n increases, the number of empty time slots decreases. The duration of an empty time slot is 9 μs, while the duration of a time slot with a successful data transmission (or with an unsuccessful data transmission) is a few hundred micro seconds. Because of this, as the number of active nodes n increases, the time period required for an active node to successfully transmit a data frame (and to be allocated a backoff count selected from the newly adjusted contention window) increases. This means the settling time after adjustment will increase with the number of active nodes n. Provided the network parameter values shown in Table I and given a value of n in the range $[2, 40]$, the value 500 ms of contention window adjustment time interval Δt corresponds to more than 2,000 time slots. The value 500 ms is large enough compared to the settling time period, since the settling time period when the number of active nodes n is 40 requires less than a few hundred time slots.

4) Analysis Results: The probability distribution P^j_i is obtained from equations (5)-(6), and the network total throughput can be obtained from equations (23)-(25) in [15]. Fig. 10 shows analytical results on the throughput performance with different convergence time period values, i.e. 2 seconds and 120 seconds. We see in the figure that when the convergence time is equal to 2 seconds, the throughput gain of AVBA outperforms that of CRB as the number of active nodes n increases above 15. This is because a network using AVBA achieves a collision free state within a short convergence time. In the range $[2, 14]$, the maximum throughput when using AVBA is slightly lower than the maximum throughput when using CRB. This is because AVBA tends to generate a backoff count larger than a backoff count generated by VBA, and it causes a larger number of idle time slots. However, Fig. 11 presents analytical results showing that the convergence time period when using VBA rapidly increases with the number of active nodes, while it slowly increases when using AVBA.

TABLE I: Parameters used for numerical analysis.

Parameters	Value
Bit rate for Data frames	54 Mbps
Bit rate for ACK frames	6 Mbps
UDP payload	1400 bytes
UDP header + IP header	28 bytes
empty time slot interval	9 μs
SIFS time interval	16 μs
DIFS time interval	34 μs
MAC header	34 bytes
Preamble signal duration	16 μs
PLCP header duration	4 μs
W_0	16
W_m	1024
Adjustment time interval Δt	500 ms

VI. SIMULATION RESULTS

We have developed a Monte Carlo network simulation to test the practicality of AVBA and to validate the numerical analysis in the previous section. The simulation parameters are summarized in Table II. Fig. 12 shows four different simulation configurations. In Setup-A, B, and C, a data rate of 54 Mbps is used by stations for sending data packets, while in Setup-D a data rate of 18 Mbps is used; all ACK frames are transmitted at 6 Mbps. Distance values between the AP and stations are selected from a triangular distribution in the range [2, 5] meters, and the simulation is repeated 100 times. In this Monte Carlo simulation, stations are uniformly placed within the two-dimensional circular space. The maximum range of 5 meters is small enough to guarantee a successful data frame transmission when a packet collision does not occur.

In Setup-A described in Fig. 12a, all the active nodes operate using AVBA, while in Setup-B shown in Fig. 12b active nodes using AVBA coexist with active legacy DCF nodes. The two APs in Setup-C described in Fig. 12c are placed at a distance L from each other, and they are assumed to use the same frequency channel. Each of the APs has 10 connected stations, assumed to use the same frequency channel as well. So, transmitted signals from nodes connected to one AP may interfere with transmitted signals from nodes connected to the other AP. In this setup, the Nakagami fading model [20] is used along with a log distance propagation loss model (exponent=3) in order to obtain realistic simulation results. Lastly, in Setup-D shown in Fig. 12d, the location of STAs 1-3 is fixed at 110 meters away on the leftside from the

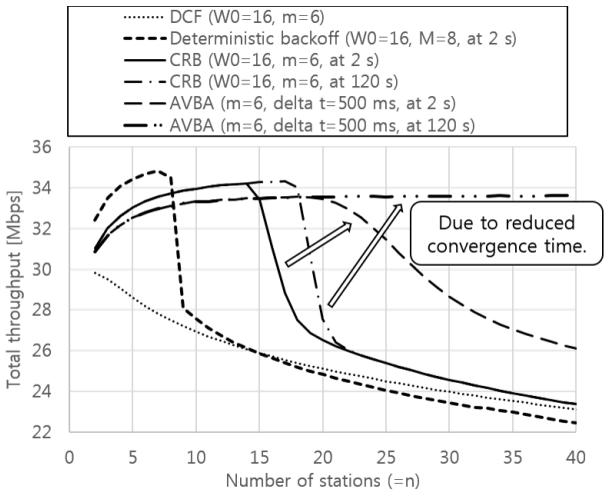

Fig. 10: The relation of the number of active nodes n, convergence time and network saturation throughput.

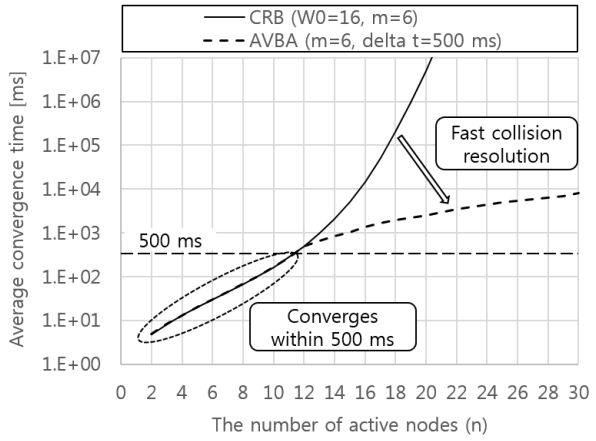

Fig. 11: Average convergence time when Δt = 500 ms.

TABLE II: Simulation parameters.

Parameters	Value
Wireless standard	IEEE 802.11a PHY
Frequency channel	5.0 GHz
Bandwidth	20 MHz
Propagation loss model	Log distance model (exponent=3)
Transport layer protocol	UDP
UDP payload length	1400 bytes
MCS for ACK frame	BPSK with a rate $\frac{1}{2}$ coding
Available data rates	6, 9, 12, 18, 24, 36, 48, and 54 Mbps
Transmission queue	Single queue
Traffic model	Full buffer
Tx power	16 dBm
Rx sensitivity	-91 dBm
W_0	16
W_m	1024
BER model	Reference [18]
CW adjustment time interval Δt	500 ms

AP, while the location of STA 4 (i.e. the notation L) changes on the right side. The distance L in Setup-C and Setup-D is given as equation (7),

$$L = d + x \tag{7}$$

where the scalar d represents an integer and x denotes a random number selected from a Normal Distribution with zero mean and unit variance. The simulation is repeated 100 times, and we obtain average values. In Setup-C, the value d varies from 5 to 500 metres, and we observe how the total throughput per AP changes. In Setup-D, the value d changes from 2 to 220 metres, and we find how the network throughput performance will change when STA 4 becomes a hidden node (to the three nodes in the opposite side) at a distance.

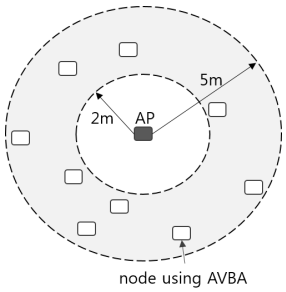

(a) Setup-A: Only AVBA nodes.

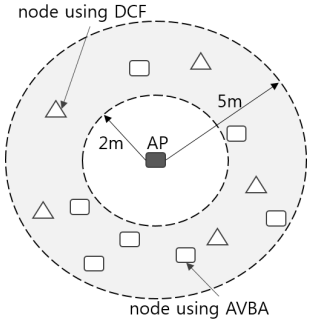

(b) Setup-B: Mixed nodes.

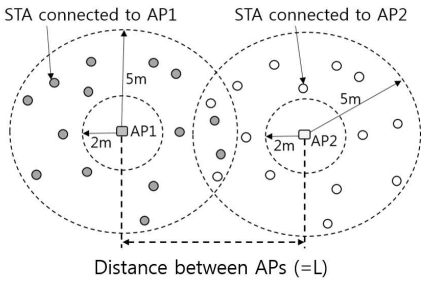

(c) Setup-C: Two access points overlapped. (Note that $L = d + x$, where x is a random variable.)

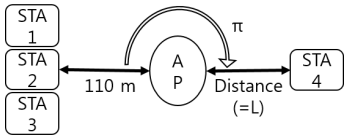

(d) Setup-D: A hidden node. (Note that $L = d + x$, where x is a random variable.)

Fig. 12: Two-dimensional setups.

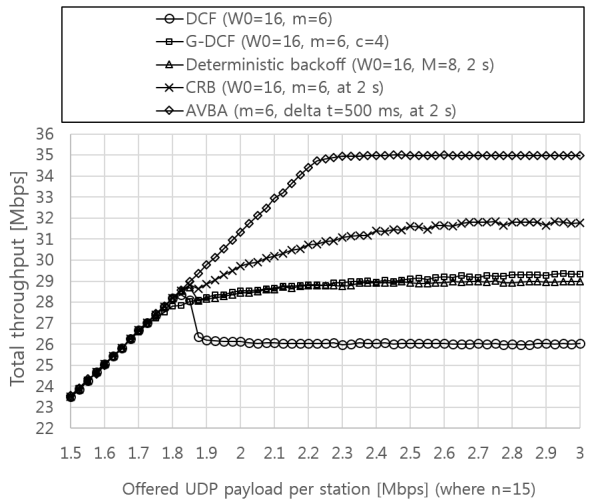

Fig. 13: Relation between total throughput and offered UDP payload per node.

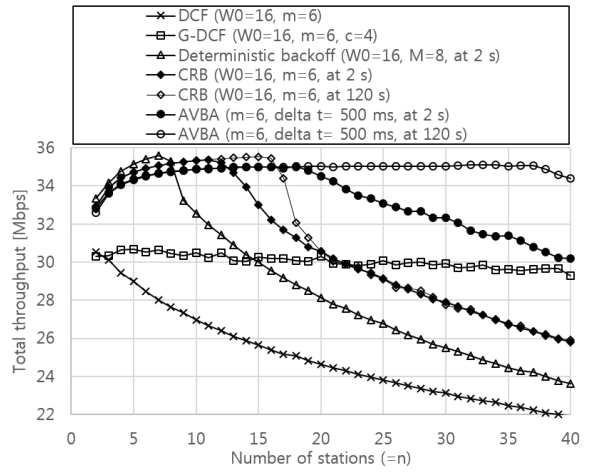

Fig. 14: Relation between total throughput and the number of active stations.

A. Results in Setup-A

Fig. 13 and Fig. 14 show simulation results on the total throughput when using the DCF, G-DCF, deterministic backoff, CRB, and AVBA. Fig. 13 shows the total throughput when using AVBA with 15 active stations increasing up to 35 Mbps as the offered payload per station increases. In Fig. 14, the total throughput performance when using DCF rapidly decreases with the number of active nodes n, while when using G-DCF the throughput performance very slowly decreases as the value n increases within the range [2, 40]. The maximum total throughput value that is achieved by G-DCF is about 30 Mbps. (In this simulation, nodes using G-DCF halve their contention window size after the fourth consecutive successful transmission.) The other three methods that achieve a collision free state, i.e. deterministic backoff (the deterministic value in this simulation is $W_0/2$), CRB, and AVBA, demonstrate a higher total throughput within the plotted range for n. The maximum total throughput value that is achieved in a collision free state is about 34-35 Mbps. We see that when two seconds of the convergence time have passed, the throughput performance when using AVBA outperforms that of using CRB when n is in the range $[14, 40]$. It is also observed that when 120 seconds of convergence time have passed, AVBA achieves a throughput of 35 Mbps or so regardless of n within the plotted range. When the value n is 30, the total throughput of AVBA after 120 seconds outperformed that of CRB by 27%. These total throughput results closely match with the analytical results presented in Fig. 10.

Fig. 16a shows the total throughput results when the number of active nodes n increases by 5 users every 5 seconds, and Fig. 16b shows the results when n increases by 5 users every 60 seconds. In Fig. 16a, when the number of active nodes n becomes 15 for the 10-15 seconds time period, the throughput performance of AVBA becomes higher than that of the other methods. As the value n increases over 15 up to 60, the throughput performance still outperforms that when using CRB. In Fig. 16b, when the value n becomes 20 for the 180-240 seconds time interval, the throughput performance of AVBA becomes higher than that of the other methods. As the value n increases over 20 up to 60, the throughput performance still outperforms that when using CRB. This is because the adaptive virtual contention window size in AVBA increases with the number of synchronized nodes in the cell, and this reduces the number of packet collisions.

B. Results in Setup-B

Fig. 15 shows the throughput performance in the mixed network setup described in Fig. 12b, where the total number of active nodes is 10, i.e. the number of active AVBA nodes plus the number of active legacy DCF nodes is equal to 10. Fig. 15a shows that the gap of throughput per node between a node using AVBA and a legacy DCF node is smaller than that of between a node using CRB and a legacy DCF node. This throughput gap is also smaller than that between a node using the deterministic backoff method and a node using the legacy DCF protocol. This is because AVBA allocates more empty time slots, as the proportion of AVBA nodes increases. Fig. 15b shows that the Jain's fairness index (JFI)[1] of the mixed network is improved. This result means that AVBA is fairer to legacy DCF nodes than VBA or deterministic backoff. Note that the throughput gap gradually increases as the proportion of nodes using AVBA increases.

Fig. 15c shows that the total network throughput in the mixed network gradually increases as the proportion of AVBA nodes increases. We also see that the total throughput when using AVBA is very close to that when using CRB. In addition, the figure shows that the total throughput when using either CRB or AVBA is higher than that when using the deterministic backoff method. This gap of throughput gain is due to the fact that in the deterministic backoff method, nodes tend to reserve a unique time slot through real packet collisions, while in CRB or AVBA the nodes can be allocated a unique time slot through virtual collisions which only conceptually occur in the algorithms.

[1]JFI is a metric to determine if nodes in a network are receiving a fair share of communication resources.

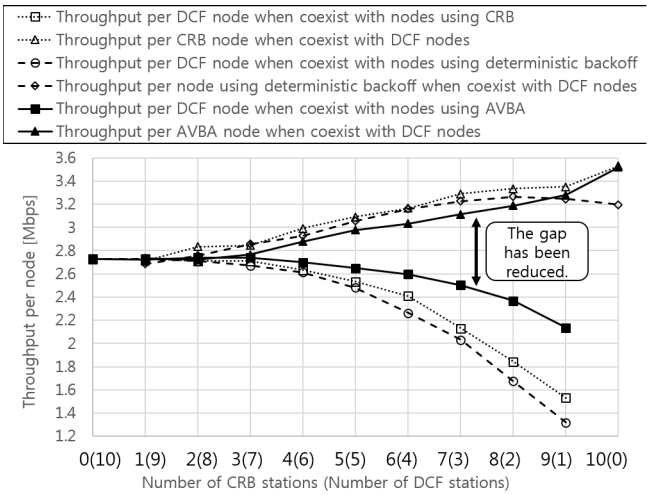

(a) Throughput per node in the mixed network (n=10).

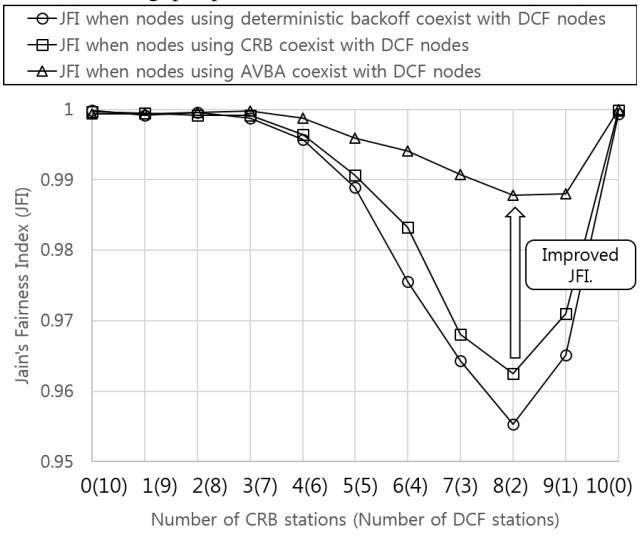

(b) Jain's fairness index (JFI).

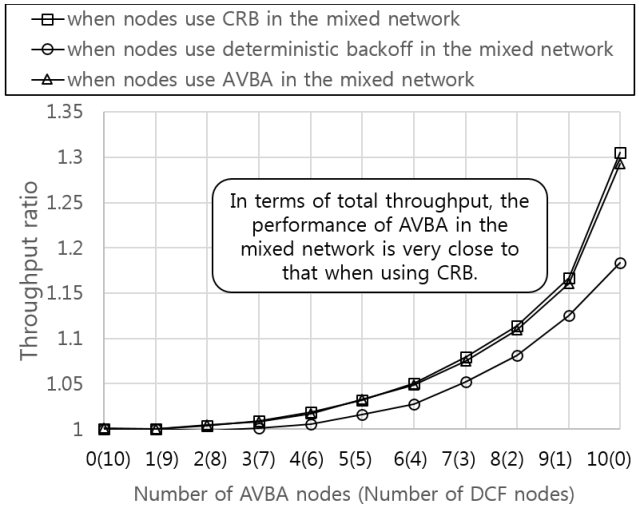

(c) Total throughput performance compared to that when using legacy DCF network with $n = 10$.

Fig. 15: Simulation results in the mixed network setup.

C. Results in Setup-C

The wireless medium in Setup-C is shared by two wireless networks, each of which has 10 active nodes using the same frequency channel. Transmitted signals from nodes connected to one AP may interfere with transmitted signals from nodes connected to the other AP. Fig. 17 shows that as the distance increases, the total throughput per AP increases. This is because the strength of interference signals from the other network is reduced by propagation loss, as the distance value increases. Note that the throughput performance when using AVBA is very close to that when using the legacy DCF protocol in the range [5, 200]. This is because nodes using AVBA tend to revert back to the DCF protocol as transmission failure increases, i.e. they independently select a random value for their backoff count (like a legacy DCF node) after a transmission failure.

D. Results in Setup-D

Fig. 18 shows the total throughput in Setup-D as the distance d increases. In this setup, all stations use a data rate of 18 Mbps, and the maximum total throughput achieved in a collision free state is about 15 Mbps. The results show that the hidden node problem occurs when the value d varies in the range $d \in [92, 128]$ causing a significant loss in throughput. In this range, we see that the throughput performance when using AVBA is only slightly higher than that when using the legacy DCF method.

In this simulation, as denoted in the figure where the range $d \in [0, 50]$, we can observe the capture effect that can occur when STA4 and one (or more than one) of STAs 1-3 transmit simultaneously. When STA4 is located within this range, the received signal from STA4 becomes much stronger than signals from STAs 1-3. Because of this capture effect, the total throughput in the range $d \in [0, 50]$ is slightly higher compared to that when the capture effect does not occur in the range $d \in [60, 80]$.

VII. CONCLUSIONS AND FUTURE WORK

This paper proposed the adaptive virtual backoff algorithm for achieving collision free wireless networks while maintaining compatibility to legacy nodes using the standard DCF protocol. The evaluation results showed that it improves the convergence speed compared to CRB, and when 120 seconds convergence time has passed the total throughput performance of the network with 30 active nodes is improved by 27 %. Moreover, the simulation results showed that regardless of the proportion of nodes using AVBA in the mixed network configuration, the fairness index is maintained above 0.98. However, when using CRB, the Jain's fairness index decreases below 0.98 when the proportion of CRB nodes increases above 0.6. Because of these results, AVBA is a more effective collision resolution technique and more fairly coexists with existing WLANs. Since the proposed technique has some features of both decentralized and centralized scheduling methods, it could be used for fair and efficient femto-cell (or small-cell) communications operating in unlicensed frequency bands.

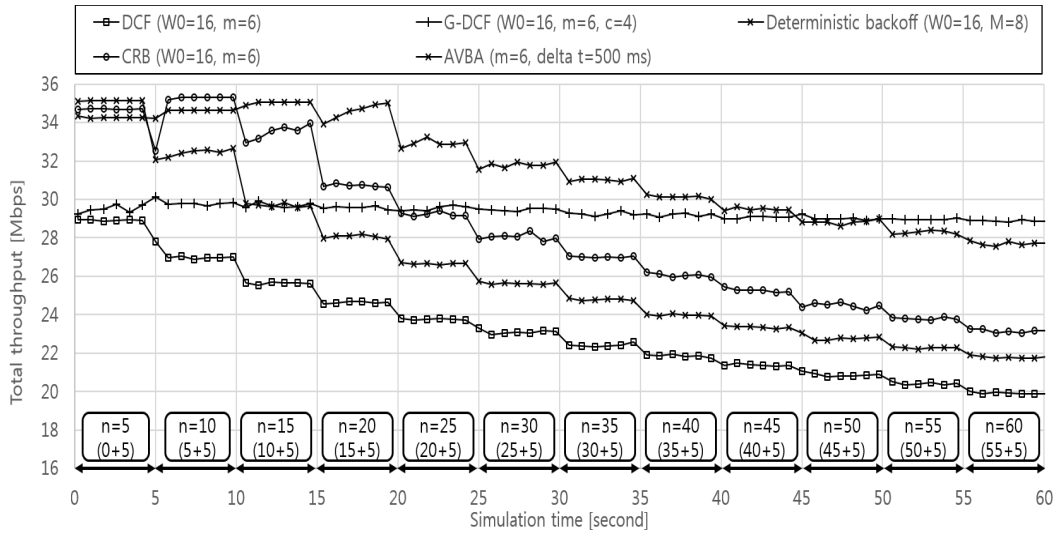

(a) Simulation results when the number of active nodes n increases by 5 every 5 seconds.

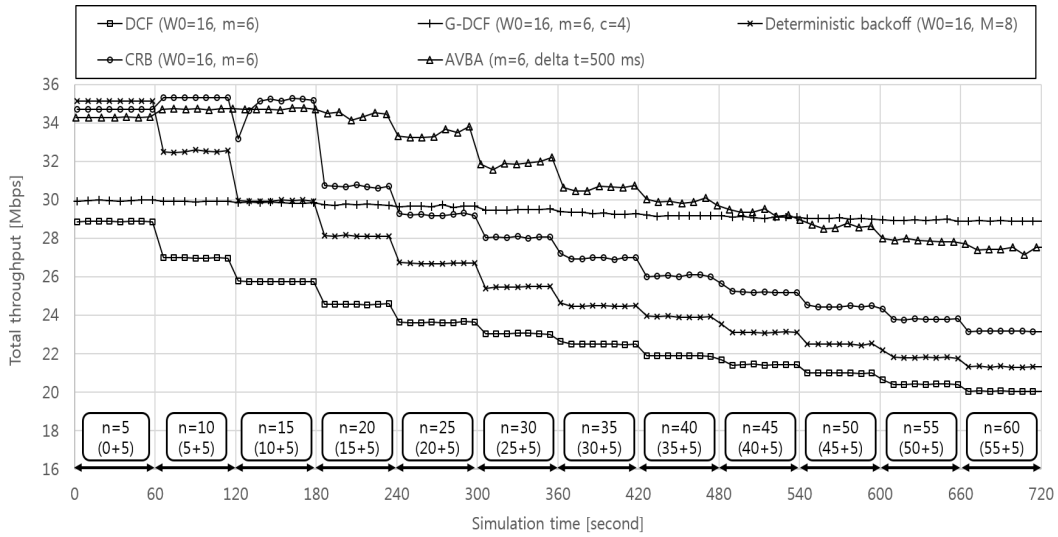

(b) Simulation results when the number of active nodes n increases by 5 every 60 seconds.

Fig. 16: Total throughput when the number of active nodes changes over time.

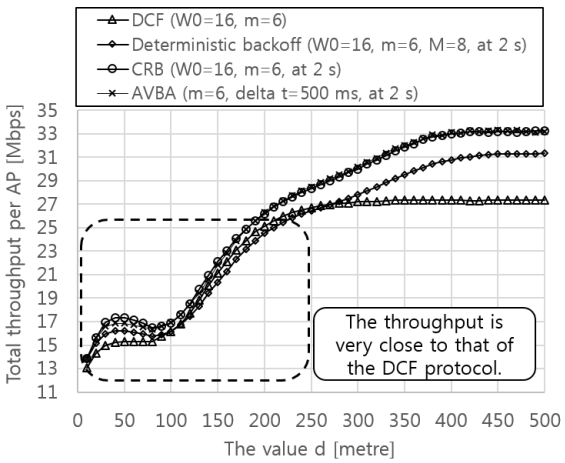

Fig. 17: Total throughput when two APs coexist. (Note in Fig. 12c, $L = d + x$, where x is a random variable.)

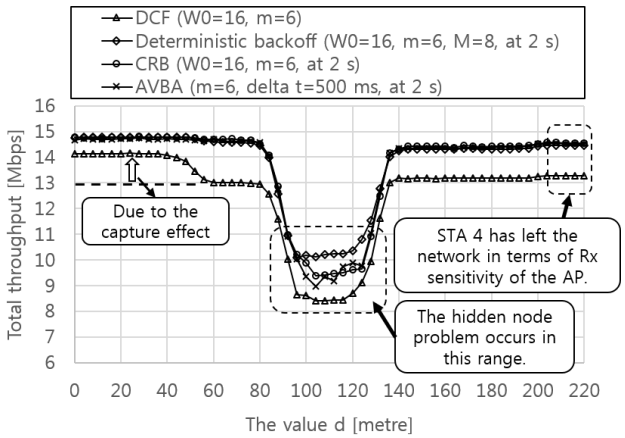

Fig. 18: Total throughput in the presence of the hidden node problem. (Note in Fig. 12d, $L = d + x$, where x is a random variable.)

As future work, the performance of AVBA in environments with a high level of interference, e.g. airports and coffee shops, should be experimentally tested. In addition, synchronization of an allocated backoff count, i.e. a SBC, between the AP and the allocated station can be disrupted by an interference signal that can be caused by the hidden node problem and the exposed node problem. The practical impact of this desynchronization issue should be investigated. In addition, the analysis model could consider more practical conditions, for example a limited number of retransmissions, imperfect channel conditions (e.g. fading channel, hidden nodes, or interference with jamming signals), support of a quality of service (QoS) control, unsaturated traffic conditions, frame aggregation with the use of a block ACK frame, and so on.

VIII. Acknowledgment

This research was funded by the EPSRC (Engineering and Physical Sciences Research Council) in United Kingdom through the Seamless and Efficient Wireless Access for Future Radio Networks (SERAN) project, grant number EP/L026147/1. All data used within this publication can be reproduced by the source code of network simulation at: https://doi.org/10.7488/ds/2508.

References

[1] F. Cali, M. Conti, and E. Gregori, "Dynamic tuning of the IEEE 802.11 protocol to achieve a theoretical throughput limit," *IEEE/ACM Transactions on Networking*, vol. 8, no. 6, pp. 785–799, Dec. 2000.

[2] C. Wang, B. Li, and L. Li, "A new collision resolution mechanism to enhance the performance of IEEE 802.11 DCF," *IEEE Transactions on Vehicular Technology*, vol. 53, no. 4, pp. 1235–1246, July 2004.

[3] J. Choi, J. Yoo, and S. Choi, "EBA: An enhancement of the IEEE 802.11 DCF via distributed reservation," *IEEE Transactions on Mobile Computing*, vol. 4, no. 4, pp. 378–390, July 2005.

[4] J. Lee and J. Walrand, "Zero collision random backoff algorithm," *IEEE INFOCOM*, 2007.

[5] Y. He, J. Sun, R. Yuan, and W. Gong, "A reservation based backoff method for video streaming in 802.11 home networks," *IEEE Journal on Selected Areas in Communications*, vol. 28, no. 3, April 2010.

[6] J. Barcelo, A. Toledo, C. Cano, and M. Oliver, "Fairness and convergence of CSMA with enhanced collision avoidance (ECA)," *IEEE International Conference on Communications (ICC)*, vol. 4, pp. 511–523, Dec. 2010.

[7] J. Barcelo, B. Bellata, C. Cano, A. Sfairopoulou, M. Oliver, and K. Verma, "Towards a collision-free WLAN: Dynamic parameter adjustment in CSMA/E2CA," *EURASIP Journal of Wireless Communications and Networking*, 2011.

[8] Y. He, J. Sun, X. Ma, A. Vasilakos, R. Yuan, and W. Gong, "Semi-random backoff: towards resource reservation for channel access in wireless LANs," *IEEE/ACM Transactions on Networking*, vol. 21, no. 1, pp. 204–217, Feb. 2013.

[9] L. Sanabria-Russo, A. Faridi, B. Bellata, J. Barcelo, and M. Oliver, "Future evolution of CSMA protocols for the IEEE 802.11 standard," *IEEE International Conference on Communications (ICC)*, 2013.

[10] L. Sanabria-Russo, F. Gringoli, J. Barcelo, and B. Bellalta, "Implementation and experimental evaluation of a collision-free MAC protocol for WLANs," *IEEE International Conference on Communications (ICC)*, 2015.

[11] S. Misra and M. Khatua, "Semi-distributed backoff: Collision-aware migration from random to deterministic backoff," *IEEE Transactions on Mobile Computing*, vol. 14, no. 5, pp. 1071–1084, Jan. 2015.

[12] M. Tuysuz and H. Mantar, "Exploiting the channel using uninterrupted collision free MAC adaptation over IEEE 802.11 WLANs," *Wireless Communications and Mobile Computing*, vol. 91, pp. 1227–1230, 2015.

[13] L. Sanabria-Russo, J. Barcelo, B. Bellalta, and F. Gringoli, "A high efficiency MAC protocol for WLANs: Providing fairness in dense scenarios," *IEEE/ACM Transactions on Networking*, vol. 25, no. 1, pp. 492–505, Feb. 2017.

[14] J. Kim, D. Laurenson, and J. Thompson, "Fair and efficient full duplex MAC protocol based on the IEEE 802.11 DCF," *IEEE International Symposium on Personal, Indoor, and Mobile Radio Communications (PIMRC)*, vol. 90, pp. 538–548, Mar. 2016.

[15] ——, "Centralized random backoff for collision resolution in Wi-Fi networks," *IEEE Transactions on Wireless Communications*, vol. 16, no. 9, pp. 5838–5852, Sep. 2017.

[16] G. Bianchi and I. Tinnirello, "Kalman filter estimation of the number of competing terminals in an IEEE 802.11 network," *IEEE INFOCOM*, 2003.

[17] A. Toledo, T. Vercauteren, and X. Wang, "Adaptive optimization of IEEE 802.11 DCF based on Bayesian estimation of the number of competing terminals," *IEEE Transactions on Mobile Computing*, vol. 5, no. 9, pp. 1283–1296, Sept. 2006.

[18] M. Lacage and T. Henderson, "Yet another network simulator," *ACM Proceeding from the 2006 workshop on NS-2: the IP network simulator*, 2006.

[19] G. Bianchi, "Performance analysis of the IEEE 802.11 distributed coordination function," *IEEE Journal on Selected Areas in Communications*, vol. 18, no. 3, pp. 535–547, Mar. 2000.

[20] M. Stoffers and G. Riley, "Comparing the ns-3 propagation models," *IEEE International Symposium on Modeling, Analysis and Simulation of Computer and Telecommunication Systems*, 2012.

Jinho D. Kim was born in Daegu, South Korea, in 1983. Since Jan. 2019, he has been working with Hyundai Motor Company, South Korea. He received the Global Top Talent Scholarship from Hyundai Motor Group, South Korea, during 2018. From Jan. 2018 to Dec. 2018, he participated in the SERAN project as a Research Associate of the University of Edinburgh, Scotland, UK. He received the PhD degree from the School of Engineering, University of Edinburgh, UK, July 2018. During the PhD course, he proposed the concept of centralized random backoff for fair and efficient wireless networks. During 2009-2014, he worked with LG Electronics, Seoul, South Korea, and participated in standardization groups, such as the IEEE 802.11ah/ax and the Wi-Fi Alliance. Currently, his interests lie in fair and efficient resource scheduling methods in wireless communications.

Dave I. Laurenson is currently a Senior Lecturer at The University of Edinburgh, Scotland. His interests lie in mobile communications: at the link layer this includes measurements, analysis and modelling of channels and MAC protocols, whilst at the network layer this includes provision of mobility management and Quality of Service support. His research extends to practical implementation of wireless networks to other research fields, such as prediction of fire spread using wireless sensor networks, deployment of communication networks for distributed control of power distribution networks, and sensor networks for environmental monitoring and structural analysis.

John S. Thompson is currently a Professor in Signal Processing and Communications at the School of Engineering in the University of Edinburgh. He specializes in antenna array processing, cooperative communications systems and energy efficient wireless communications. He has published in excess of three hundred papers on these topics, including one hundred journal paper publications. He is currently the project coordinator for the EU Marie Curie International Training Network project ADVANTAGE, which studies how communications and power engineering can provide future ”smart grid” systems. He was an elected Member-at-Large for the Board of Governors of the IEEE Communications Society from 2012-2014, the second largest IEEE Society. He is also a distinguished lecturer on the topic of energy efficient communications and smart grid for the IEEE Communications Society during 2014-2015. He is an editor for the Green Communications and Computing Series that appears regularly in IEEE Communications Magazine. In January 2016, he was elevated to Fellow of the IEEE for contributions to multiple antenna and multi-hop wireless communications.